A MODIFIED DUAL-WAVELENGTH TECHNIQUE FOR KU- AND KA-BAND RADAR RAIN RETRIEVAL

Liang Liao[1] and Robert Meneghini[2]

[1] Goddard Earth Science Technology & Research, Morgan State University, MD
[2] NASA Goddard Space Flight Center, Greenbelt, MD

ABSTRACT

A modified dual-wavelength radar technique is described in an attempt to eliminate double solutions of DSD that the standard dual-wavelength technique faces for small-to-moderate rain rates. Assessment of the methods is made from the simulated hydrometeor profiles comprised of measured DSD. Preliminary results reveal that the modified radar technique has potential to improve accuracy of DSD and rain retrieval over the standard dual-wavelength radar technique.

Index Terms— Air/Space-borne radar, rain, DSD

1. INTRODUCTION

The Dual-wavelength Precipitation Radar (DPR) operating at Ku- and Ka-band, aboard the Global Precipitation Measurement (GPM) core satellite, is the first dual-wavelength radar in space [1]. An important goal of the DPR is to derive rain rate by estimating parameters of the raindrop size distribution (DSD) that is often modeled by an analytical function, such as the gamma with two or three unknown parameters. Several dual-wavelength radar retrieval techniques have been developed, many of which are based on the standard dual-wavelength technique that uses the differential frequency ratio (DFR), i.e., the difference of radar reflectivities between two wavelengths, to first infer the DSD parameters, correct attenuation and then derive rain rate gate by gate either along the radar beam (forward approach) or in the reverse direction (backward approach). To improve robustness of the dual-wavelength retrieval, a few optimal methods have been recently proposed in which one or more adjustment factors are used to modify some nominal relationships between radar and hydrometeor's parameters (such as k-Z and R-D_m relations, where k, Z, R and D_m are specific attenuation, radar reflectivity, rain rate and mass-weighted diameter) to account for DSD variation in space and time [2][3]. Adjustment factors at each gate/profile are determined by optimizing predefined cost functions that tend to satisfy dual-wavelength reflectivities and measured path integral attenuations (PIA).

The DFR-based standard dual-wavelength technique is in principle capable of accounting for spatial and temporal DSD variations, and is therefore advantageous over other approaches that rely on optimization methods. However, this is true only if there exist unique solutions of DSD to dual-wavelength radar equations. For the gamma DSD model, double solutions of D_m occur, as derived from the Ku- and Ka-band DFR, for light-to-moderate rain rates. Moreover, there is no additional information aiding in selection of the solution. As a result of this, the standard dual-wavelength technique becomes problematic for the rain retrieval if double solutions exist. Retrieval errors caused by improper selection of the solution worsen as retrieval proceeds deep into the storm as a result of error propagation. It has been found from a large collection of the measured DSD data taken from various NASA-sponsored field campaigns that double values of D_m happen for the majority of the DSD measurements, adversely affecting to a great extent the overall performance of the Ku- and Ka-band profiling retrieval of rain and DSD parameters.

To circumvent the double-value problem of D_m, a modified version of DFR, or modified DFR, denoted by DFR*, is introduced in this study. Instead of weighting equally the Ku- and Ka-band reflectivities to the DFR equation, the DFR* weights the Ka-band reflectivity less than the Ku-band so that the possibility of double solutions no longer exist. Removal of the double values of D_m by using DFR* is beneficial for lessening the ambiguities in the estimates of D_m, but the trade-off is that the DFR* is no longer exclusively a function of D_m if the gamma DSD model is assumed with the shape factor that is either fixed or constrained. This situation is different from that which uses the DFR since this depends solely on D_m. In this study, our focus is on examining the potential of DFR* for the retrieval of the vertical rain and DSD profiles by employing measured DSD data. For understanding the uncertainties in rain rate estimation and in gaining insight into ways to improve the profiling algorithms, a physical evaluation of the standard (DFR-based) and modified (DFR*-based) dual-wavelength techniques is conducted by applying them to simulated vertical rain profiles. To construct realistic hydrometeor profiles used for our evaluation, the measured DSD data acquired from a variety of storm systems are used. To test the algorithms for various degrees of vertical

rain inhomogeneity, generated hydrometeor profiles are grouped into the categories with various vertically spatial correlations, i.e., from perfectly correlated to partially correlated DSD profiles. Performance of rain estimates using standard and modified dual-wavelength radar techniques is investigated by comparing the radar and hydrometeor parameters retrieved with those directly derived from DSD measurements. The DSD data that are used include the multiple Parsivel[2] observations acquired during the Iowa Flooding Studies (IFloodS), the Integrated Precipitation Validation Experiment (IPHEx) and data from NASA Wallops Flight Facility in Wallops Island, Virginia as well as the Olympic Mountains Ground Validation Experiment (OLYMPEX) field campaign.

2. MODIFIED DUAL-λ RADAR TECHNIQUE

The modified dual-wavelength technique, denoted by DFR*, is expressed as

$$DFR^* = 10\log_{10}\left(\frac{Z_{Ku}}{\gamma Z_{Ka}}\right), \quad (1)$$

where γ is a scale and weighting factor with a value ranging from 0 to 1. The definition of DFR* in above equation could also possibly be viewed as a generalized form for the dual-wavelength applications due to the fact that it can switch easily from single wavelength with γ=0 to the standard dual-wavelength methods with γ=1. With the γ value less than 1 the Ka-band radar reflectivity is partially weighted in the DFR* equation. Unlike the DFR, the DFR* is generally dependent on N_w.

Figure 1 illustrates an example of the D_m-DFR* relations and their comparisons as γ takes on different values. The scatter plots are the results derived from the DSD data with the colors representing different N_w values. The thick black solid lines are the means of the data points. Theoretical computational results (blue curves) are plotted from the gamma DSD model with a fixed μ of 3 as N_w varies from 10 to 10^5 $mm^{-1}m^{-3}$. For reference, the contours of Z_{Ku} in dBZ (red curves) are also plotted. Shown in the top-left panel is the case for the single Ku-band, i.e., γ=0, while the results from the standard dual-wavelength technique (γ=1) are shown in the bottom-right panel. The cases where γ equals to 0.5 and 0.7 are displayed in the top-right and bottom-left panels, respectively. Several interesting features are revealed in Fig.1; in particular, that D_m has a one-to-one relation with DFR* for all the cases shown in the plots except for one case, i.e., γ=1. As expected, the D_m-DFR* relations depend on N_w if γ is not 1, and the degree of dependence on N_w depends on γ. The strongest dependence of N_w on these relations occurs at γ=0 (Ku-band only), as shown from both the DSD-derived data points and the model computations. Variability in the D_m-DFR* with respect to N_w tends to decrease as γ increases. The DFR* at γ=1, or the standard DFR, is independent of N_w. It is worth

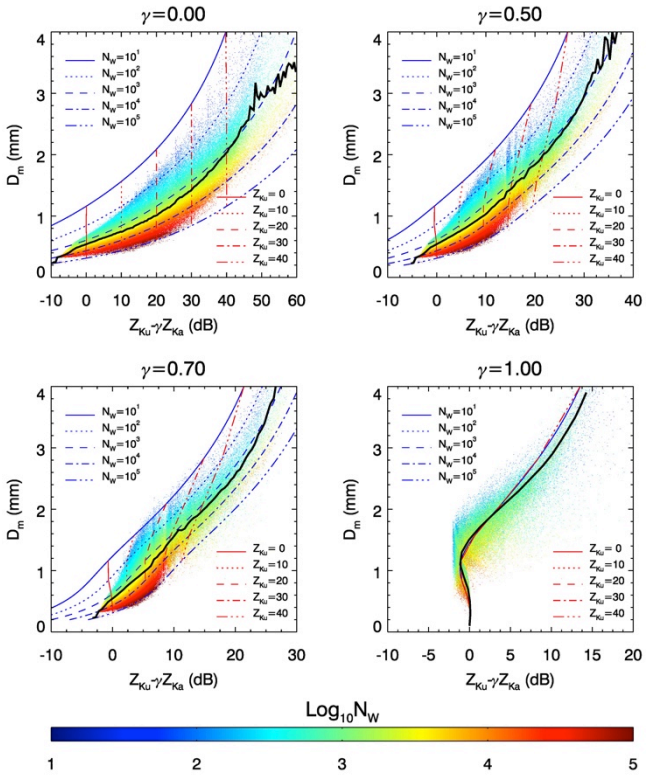

Fig.1 Scatterplots of D_m versus modified DFR as derived from the DSD data for the cases of the weighting factor γ of the modified DFR equal to 0, 0.5, 0.7 and 1. Colors of the data points depict N_w values that derived from the same DSD data. The mean values of the data are given in the thick dark curves. Theoretical model computations, represented by blue and red curves, are provided as the DSD is modeled as the gamma distributions with a fixed μ of 3 and N_w ranging from 10 to 10^5 in $mm^{-1}m^{-3}$. Contours of Z_{Ku} at the values from 0 to 40 dB (red curves) are plotted as well for reference.

reiterating that one of the crucial differences between the DFR* (γ≠1) and the standard DFR is that the former gives a unique solution to D_m while the latter results in double values of D_m for most of the radar measurements. Similar behavior is also found in the rain rate estimates (not shown). Unique solutions to D_m and rain rate to the DFR* are perhaps the most desirable features from the perspective of radar retrievals, but it doesn't come without a cost. In fact it is at the expense of adding the variable N_w to the retrieval equations, leading to the a retrieval under-constraint.

To retrieve rain and DSD profiles using DFR*, one simple way is to assign the same N_w to the entire vertical range gates as an initialization process. With known N_w, D_m can be uniquely derived by the DFR*; rain rate and attenuation coefficients can then be derived by using DFR* along with Z_{Ku}. Attenuation corrections to the measured radar reflectivity profiles are carried out consecutively gate-by-gate along the radar beam either in the forward or

backward direction. The derived hydrometeor profiles depend on the value of N_w assumed. How to find proper N_w that leads to accurate DSD and rain profiles is a key in the retrieval procedures.

In the search for N_w, an optimization method is employed in an attempt to minimize the discrepancies of the simulated and measured radar parameters. Mathematically, N_w is selected to maximize the product of the following three probability functions (or constraints) for given a series of initial values of N_w, denoted by $\tilde{N}_{w,k}$, where k=1, 2, …, K (where K is the total number of the initial tests of N_w),

$$p_1(N_w)p_2(N_w)p_3(N_w) = \max\left(p_1(\tilde{N}_{w,k})p_2(\tilde{N}_{w,k})p_3(\tilde{N}_{w,k})\right) \quad (2)$$

where

$$p_1(\tilde{N}_{w,k}) = \frac{1}{\sigma_1\sqrt{2\pi}}\exp\left(-\frac{(\log_{10}\tilde{N}_{w,k}-3.45)^2}{2\sigma_1^2}\right),$$

$$p_2(\tilde{N}_{w,k}) = \frac{1}{\sqrt{2\pi}}\exp\left(-\frac{(\delta PIA(\tilde{N}_{w,k})-\delta PIA_{SRT})^2}{2\sigma_2^2}\right),$$

$$p_3(\tilde{N}_{w,k}) = \prod_{n=1}^{N}\frac{1}{\sqrt{2\pi}}\exp\left(-\frac{(Z_{m,n,est}^{(Ka)}(\tilde{N}_{w,k})-Z_{m,n,obs}^{(Ka)})^2}{2\sigma_3^2}\right)$$

where δPIA is the differential PIA defined as difference of PIA between Ka- and and Ku-band, $Z_{m,n,est}^{(Ka)}(\tilde{N}_{w,k})$ and $Z_{m,n,obs}^{(Ka)}$ are respectively the simulated and measured Ka-band apparent radar reflectivities at the nth range gate. Function $p_1(\tilde{N}_{w,k})$ describes the distribution of $\log_{10}(N_w)$ that has a mean of 3.45 and standard deviation σ_1, derived from the DSD data. $p_2(\tilde{N}_{w,k})$ reflects differences of δPIA between the simulations and the SRT estimates while $p_3(\tilde{N}_{w,k})$ accounts for discrepancies of the simulated and measured Ka-band reflectivities. σ_2 acts as a weighting factor, changing with the SRT accuracy (or reliability). σ_3 is constant and its value could possibly be optimized through the retrieval evaluation processes. It should be noted that the SRT-estimated δPIA has much less variance than either PIA(Ku) or PIA(Ka) derived by the SRT because of strong correlation of the normalized surface cross section (σ^0) between Ku- and Ka-band [4].

A flowchart is provided in Fig.2 to show the forward approach in estimates of radar and DSD parameters gate by gate as $\text{Log}_{10}(\tilde{N}_{w,k})$, k=1, 2, …, K, is equally spaced in the range from 1 to 10^6 $\text{mm}^{-1}\text{m}^{-3}$. The selected N_w is among $\text{Log}_{10}(\tilde{N}_{w,k})$, k=1, 2, …, K, and it satisfies Eq.(2). Retrieved rain and D_m profiles are those solutions that correspond to the selected N_w. Similar job can be done for the backward approach retrieval.

3. PRELIMINRY RESULTS

For evaluation of the modified dual-wavelength technique and its comparisons with the standard DFR

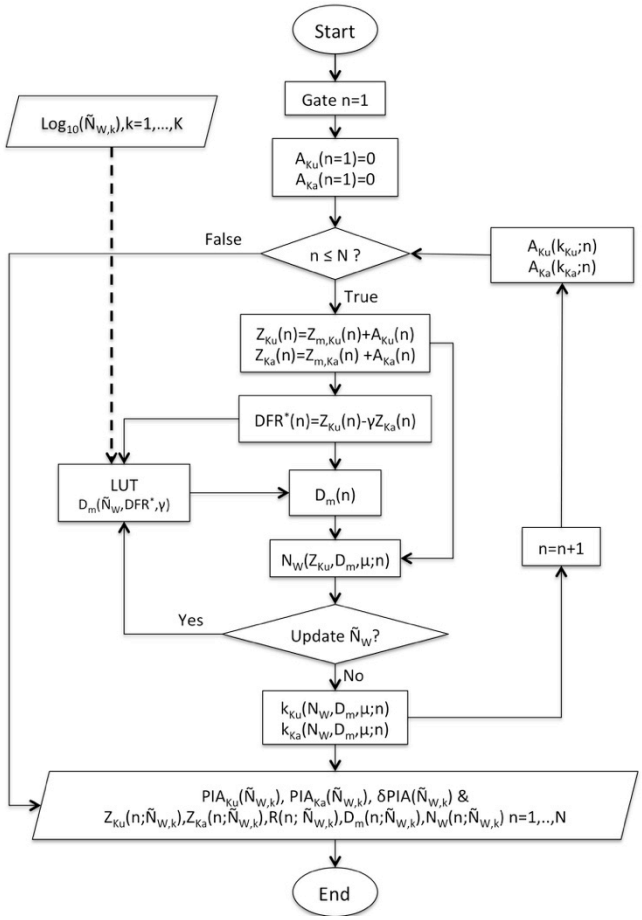

Fig.2 Flowchart of the modified dual-wavelength technique (DFR*) for retrieval of DSD parameters and rain rate.

algorithm, the measured DSD data acquired from a variety of storm systems during the NASA field campaigns are used to construct realistic hydrometeor profiles from which the retrieval is carried out. Two types of vertical DSD profiles are created: One is vertically uniform DSD profile, i.e., a single DSD is used for entire column, and another is the non-uniform profile in which DSD varies gate by gate along the column. The range resolution is 0.125 km, comparable to the case for the GPM DPR, and rain height is set at 5 km. To construct realistic non-uniform hydrometeor profiles, the time-series DSD data are converted to the vertical profiles by assigning 1-minute-integration-time DSD to the gates from the top to surface consecutively. With the DSD spectra both radar and hydrometeor's parameters can be accurately computed, including true and measured radar reflectivities, attenuation, rain and DSD characteristic parameters (D_m and N_w). These DSD-based calculated parameters serve as truth. An evaluation of algorithm performances is conducted by comparing the radar estimates with the truth.

Shown in Fig.3 are the results of the comparisons of D_m (upper panel) and rain (lower panel) retrieved by the

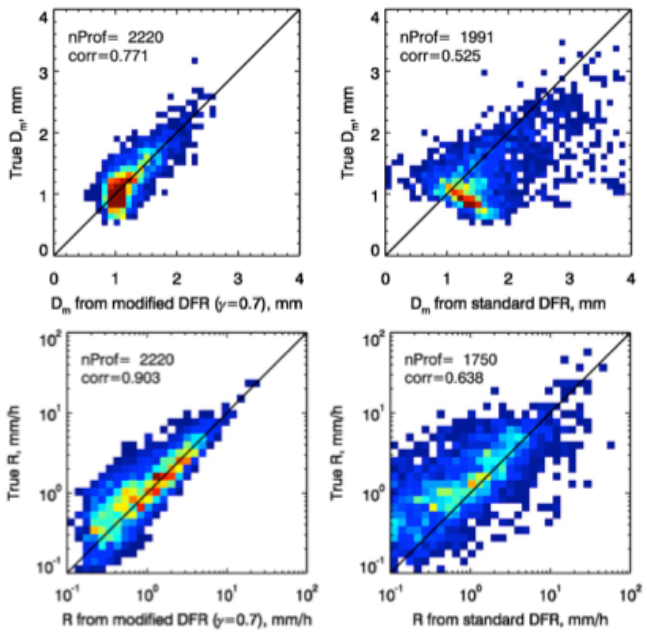

Fig.3 Comparisons of D_m (top) and rain (bottom) estimated by the modified DFR (left) and standard DFR (right) with their truths.

modified DFR* (left column) and the standard DFR (right column) with the truth value at the surface. The retrievals are made by the forward approach for the non-uniform DSD profiles as the δPIA is modeled as a random variable with an unbiased mean and standard deviation of 0.8 dB, which is similar to what the DPR measures. It is apparent that the estimates of D_m and rain from the DFR* are far more accurate than those from the standard DFR. Similar results are obtained using the backward approach.

4. SUMMARY

The modified dual-wavelength radar scheme described in the paper appears promising in improving the performance of the rain and DSD retrievals for air/space-borne Ku- and Ka-band radar over the standard dual-wavelength technique. More studies are under the way to test the retrievals conducted under various conditions to understand their sensitivities to different errors and constraints.

ACKNOWLEDGEMENTS: This work is supported by Dr. R. Kakar of NASA Headquarters under NASA's Precipitation Measurement Mission (PMM) Grant NNH15ZDA001N-PMM. The authors also wish to thank Dr. Ali Tokay from University of Maryland Baltimore County for providing DSD data.

5. REFERENCES

[1] A. Hou, Y., R. K. Kakar, S. Neeck, A. A. Azarbarzin, C. D. Kummerow, M. Kojima, R. Oki, K. Nakamura, and T. Iguchi, "The global precipitation measurement mission," *Bull. American Meteor. Soc*., vol. 95, pp. 701-722, 2014.

[2] S. Seto, T. Iguchi and T. Oki, "The basic performance of a precipitation retrieval algorithm for the Global Precipitation Measurement mission's single/dual frequency radar measurements," *IEEE Trans. Geosci. Remote Sens*., vol., pp.5239–5251, 2013.

[3] S. Seto, S., and T. Iguchi, "Intercomparison of attenuation correction methods for the GPM dual-frequency precipitation radar," *J. Atmos. Oceanic Technol*., vol.32, pp.915-926, 2015.

[4] R. Meneghini, et al., "An initial assessment of the Surface Reference Technique applied to data from the Dual-Frequency Precipitation Radar (DPR) on the GPM Satellite", *J. Atmos. Oceanic Technol*., Vol 32, pp. 2281-2296, 2015.